

## **Transverse Polarization Effects in Hard Scattering at CLAS**

H. Avakian\*, W. Brooks, V. Burkert, L. Elouadrhiri, Y. Sharabian  
Jefferson Lab, Newport News, VA 23606

D. Crabb, R. Minehart, C. Smith  
University of Virginia, Charlottesville, VA 22903

K. Griffioen  
The College of William and Mary, Williamsburg, 23187

M. Guidal  
Institut de Physique Nucléaire, F-91406 Orsay, France

K. Joo  
University of Connecticut, Physics Department, Storrs, CT 06269, USA

P. Bosted  
University of Massachusetts Amherst, MA 01003-4525 USA

E. De Sanctis, M. Mirazita, F. Ronchetti, P. Rossi  
INFN LNF, 00044 Frascati, Italy

S. Kuhn, S. Stepanyan  
Old Dominion University, Norfolk, VA 23529

G.P.Gilfoyle  
University of Richmond, Richmond, VA 23173

K. Egiyan, N. Ivanov  
Yerevan Physics Institute, Yerevan, 375036 Armenia

V. Kubarovsky, P. Stoler  
Rensselaer Polytechnic Institute, Troy, NY 12181, USA

S. Kuleshov, O. Pogorelko  
Institute of Theoretical and Experimental Physics, 117259 Moscow, Russia

\*Contact Person

## Abstract

Electroproduction of final state photons and mesons off transversely polarized protons using a 6 GeV electron beam and the CLAS detector at Jefferson Lab will be used to measure target single-spin asymmetries. Significant azimuthal angle dependent moments were predicted in photon and pion hard exclusive as well as semi-inclusive cross sections for a transversely polarized target. Measured transverse-target single-spin asymmetries in combination with the data available from longitudinally polarized target (CLAS EG1 experiment) would allow extraction and separation of different generalized parton distributions and transverse momentum dependent distributions, eventually giving access to the orbital angular momentum of partons. This measurement would also provide a simple test of the applicability of GPD-based predictions for hard exclusive production of pions at JLAB energies.

## 1 Introduction

Deep inelastic scattering (DIS) has been used extensively in recent years as an important testing ground for QCD. Studies so far have been concentrated on a better determination of parton distribution functions (PDFs) describing momentum fraction distributions of partons in the infinite momentum frame. The use of polarization in leptonproduction provides an essential new dimension for testing QCD. Polarized quark distributions have been extracted from a combination of inclusive and semi-inclusive asymmetry data [1, 2].

At leading-twist, the quark structure of hadrons is described by three distribution functions: the number density  $q(x)$ ; the helicity distribution  $\Delta q(x)$ , and the transversity distribution  $\delta q(x)$ . Although parton distribution functions cannot be computed in perturbative QCD they are universal and do not depend on the particular hard process. Once measured in semi-inclusive DIS (SIDIS) no extra input is needed in order to compute analogous quantities in hadron-hadron collisions. However as the results from DIS suggest [3], only a fraction of the nucleon spin can be attributed to the quark spins. In recent years, PDFs were generalized to contain information not only on the longitudinal but also the transverse distributions of partons in a fast moving hadron. Much of the interest in Generalized Parton Distributions (GPDs) [4, 5] has been triggered by their potential to help unravel the spin structure of the nucleon, as they contain information not only on the helicity carried by partons, but also on their orbital angular momentum (OAM). The QCD factorization theorem has been generalized to a large group of hard exclusive processes [6],

$$\gamma^*(q) + T(p) \rightarrow \gamma(q') + T'(p'); \quad \gamma^*(q) + T(p) \rightarrow M(q') + T'(p')$$

in which a photon  $\gamma^*$  with high energy and large virtuality  $-q^2 = Q^2 > 0$  scatters off the hadronic target  $T$  and produces a final state photon  $\gamma$  or hadron  $M$ .

distribution functions		chirality	
		even	odd
twist 2	U	<b>q</b>	$h_1^\perp$
	L	<b><math>\Delta\mathbf{q}</math></b>	$h_{1L}^\perp$
	T	$f_{1T}^\perp$ $g_{1T}$	$\delta\mathbf{q}$ $h_{1T}^\perp$

Table 1: List of twist-2 TMD distribution functions accessible in SIDIS.

The leading twist GPDs defining the cross section for different final states are termed  $H^q$ ,  $\tilde{H}^q$ ,  $E^q$ , and  $\tilde{E}^q$ , and depend upon three kinematic variables:  $x$ ,  $\xi$ , and  $t$ . The variable  $\xi$  is the longitudinal momentum fraction of the transfer  $\Delta = p' - p$ ,  $t = \Delta^2$  is the overall momentum transfer in the process ( $p$  and  $p'$  are initial and final nucleon momenta). In the forward limit ( $\Delta \rightarrow 0$ ), the GPDs  $H$  and  $\tilde{H}$  reduce to the quark density distribution  $q(x)$  and quark helicity distribution  $\Delta q(x)$ , respectively. The functions  $E$  and  $\tilde{E}$  are not measurable through DIS. There is a sum rule [4] that relates the second moment of the quark helicity-independent GPDs to the fraction of the nucleon spin ( $J$ ) carried by the sum of the quark spin and OAM:

$$\int_{-1}^1 dx x (H(x, \xi) + E(x, \xi)) = 2J. \quad (1)$$

Apart from GPDs, there is another class of non-perturbative functions that carry information not only on longitudinal but also on transverse hadron structure. These are transverse momentum dependent (TMD) parton distributions [7, 8, 9, 10, 11]. If the transverse momentum  $k_T$  of partons is also included, the number of independent distribution functions at leading twist increases to six [10, 11] (three of which reduce to  $q(x)$ ,  $\Delta q(x)$  and  $\delta q(x)$  when integrated over  $k_T$ ). Because they depend on the longitudinal **and** transverse momentum, these “3-dimensional” transverse momentum dependent (TMD) functions provide a more complete picture of the nucleon structure. Relaxing the time invariance condition, two additional functions ( $f_{1T}^\perp$ ,  $h_1^\perp$ ) are permitted, bringing the total number of distribution functions to eight. The full list of twist-2 distribution functions (those that survive after the  $k_T$ -integration are denoted in boldface) contributing to the double-polarized cross section in SIDIS is shown in Table 1 (see [10]). As shown recently in Ref.[12], the interaction of the active parton in the hadron and the target spectators [13, 14, 15] (see Fig. 1) leads to gauge-invariant TMD parton distributions.

The physical picture becomes particularly intuitive after a Fourier transform from transverse momentum transfer to impact parameter, both for GPDs [16, 17, 18] and TMDs [18]. GPDs in impact parameter space or impact parameter dependent (IPD) distributions, probe partons at transverse position  $\vec{b}$  (see Fig. 2a), with the initial and final state proton localized around  $\vec{0}$  but shifted relative to each other by an amount of order  $\xi\vec{b}$ . At the same time, the longitudinal momenta of the protons and

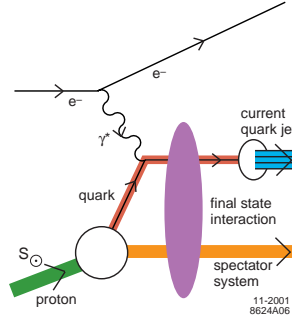


Figure 1: Interaction of struck quark and the target spectators[13].

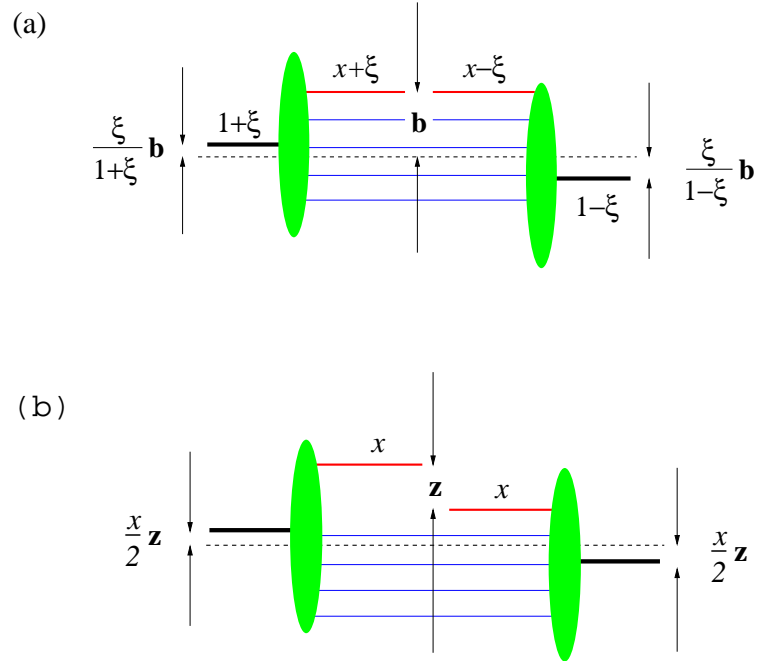


Figure 2: Representation of a GPD (a) and TMD (b) in impact parameter space [18].

hadrons are specified, in the same way as in the  $t$ -dependent GPDs. The impact parameter gives the location where a quark or antiquark is pulled out of and put back into the proton. The center-of-momentum (CM)  $\mathbf{R}_\perp$  of the target is defined by the sum  $\sum_{i \in q,g} x_i \mathbf{r}_{\perp,i}$  over the transverse positions  $\mathbf{r}_{\perp,i}$  of all quarks and gluons in the target and the weight factors  $x_i$  being the momentum fraction carried by each parton [17]. GPDs at non-zero  $\xi$  correlate hadronic wave functions with both different momentum fractions and different transverse positions of the partons. However, the difference in transverse positions is a *global* shift in each wave function; the *relative* transverse distances between the partons in a hadron are the same before and after the scattering.

In contrast to GPDs in TMD distributions (see Fig. 2b) describing the correlation in transverse position of a single parton, the struck quark has a different transverse location *relative* to the spectator partons in the initial and the final state wave functions, in addition to the overall shift of the proton center of momentum. Both TMDs  $q(x, \mathbf{k}_\perp)$  and IPDs  $q_X(x, \mathbf{b}_\perp)$  are linked to the OAM of partons and lead to predictions of single-spin asymmetries (SSA) in hard scattering processes [8, 9, 10, 11, 19, 17]. It was demonstrated recently that a non-zero OAM of partons in the nucleon is crucial in forming the target single-spin asymmetries. The interference of wavefunctions with different orbital angular momentum which may be responsible for single-spin asymmetries [8, 46, 50, 13, 14, 15, 12], also yields the helicity-flip GPD  $E(x, \xi, t)$  [20, 21] entering Deeply Virtual Compton Scattering (DVCS)[4, 5] and the Pauli form factor  $F_2$ . The helicity-flip GPD  $E(x, \xi, t)$  in impact parameter space describes how the distribution of partons in the transverse plane depends on the polarization of the nucleon and may be linked directly to various transverse SSA. A semi-classical description, based on IPD parton distributions, for polarization and single-spin asymmetries in different experiments, was presented in Ref. [17]. In case of a transversely polarized nucleon the axial symmetry is broken due to an additional contribution to the unpolarized IPD  $q(x, \mathbf{b}_\perp)$  [16]:

$$q_X(x, \mathbf{b}_\perp) = q(x, \mathbf{b}_\perp) - \frac{1}{2M} \frac{\partial}{\partial b_y} \mathcal{E}_q(x, \mathbf{b}_\perp), \quad (2)$$

where  $\mathcal{E}_q$  is the Fourier transform of the twist-2 GPD  $E_q$ . The resulting transverse flavor dipole moment is defined by the Pauli formfactor for flavor  $q$ :

$$d_q^y \equiv \int dx \int d^2 \mathbf{b}_\perp q_X(x, \mathbf{b}_\perp) b_y = \frac{1}{2M} \int dx E_q(x, 0, 0) = \frac{F_{2,q}(0)}{2M}$$

As a result of transverse distortion in transversely polarized hadrons, the flavor centers of  $u$  and  $d$  quarks were estimated to be shifted from each other  $\sim 0.4$  fm. Such a large separation between quarks of different flavors, which is both perpendicular to the momentum and spin of proton, leads to the appearance of single-spin asymmetries in hard processes.

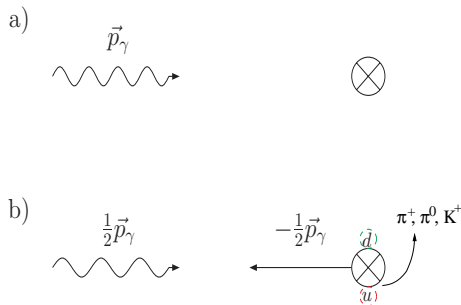


Figure 3: Photon hitting a proton target. a) laboratory frame, b) CM frame. The polarization of the proton is into the plane. The  $u$  quarks (schematically indicated by a dashed circle) are shifted down and the  $d$  quark up [17]. The produced  $\pi^+$  and  $\pi^0$  tend to go preferably up (to left if one looks into the direction of the photon momentum and the proton spin is up) assuming the final state interaction that leads to string breaking is attractive.

Measurement of the azimuthal angle distributions of observed photons and hadrons in hard exclusive and semi-inclusive leptonproduction allows access to both GPDs and TMDs[9, 13, 17].

SSA in hadronic reactions have been among the most difficult phenomena to understand from first principles in QCD. Large SSAs have been observed in hadronic reactions for decades [22, 23]. In general, such single-spin asymmetries require a correlation of a particle spin with a production or scattering plane. In hadronic processes, such correlations can provide a window to the physics of final and initial state interactions at the parton level.

Recently, significant SSAs were reported in semi-inclusive DIS (SIDIS) by the HERMES collaboration at HERA [24, 25] for a longitudinally polarized target, by the SMC collaboration at CERN for a transversely polarized target [26], and by the CLAS collaboration at JLab [27] with a polarized beam. Large beam SSA were measured in DVCS both at HERMES [28] and CLAS [29]. Single-spin asymmetry measurements opened up a unique possibility to access T-odd distribution functions in semi-inclusive DIS [13, 14]. Ongoing experiments with 6 GeV electrons at CLAS, 27.5 GeV positrons at HERMES, and 160 GeV muons at COMPASS, using various polarized and unpolarized targets will study the flavor dependence of the corresponding functions[30, 31].

It is argued that in both semi-inclusive [32] and in hard exclusive [33, 34, 35] pion production, scaling sets in for cross section ratios and, in particular, for spin asymmetries at lower  $Q^2$  than it does for the absolute cross section. There are quite a few examples of remarkable agreement between spin asymmetries measured at different beam energies over a wide  $Q^2$  range. One particular case is the very good agreement of the HERMES data with the SMC data, taken at 6-12 times higher average

$Q^2$ , showing that the semi-inclusive spin asymmetries are  $Q^2$  independent within the present accuracy of the experiments [2]. Very good agreement was observed in single-spin asymmetries in  $ep$  scattering at HERMES[36] and CLAS [38]. This makes it possible for spin-asymmetries to be a major tool for measurements of different parton distribution functions (GPDs,TMDs) in the  $Q^2$  domain of a few  $\text{GeV}^2$ .

**CLAS with a transversely polarized target would allow simultaneous measurement of beam and target SSA of final state photons (DVCS) and pseudoscalar mesons in a wide range of different kinematic variables.**

The list of other possible applications of the transversely polarized target at CLAS includes also studies of angular dependencies of pion pairs and vector meson production [39, 40]. Finally, the structure function  $g_2(x, Q^2)$  [41] could be determined from inclusive data in the JLab kinematic range.

## 2 Theoretical and Experimental issues

Operating a transversely polarized target at CLAS [42] requires some modification to the beamline and to the polarized target arrangement in CLAS. In the following we will discuss some issues of both, building a transversely polarized target at CLAS and the possible interpretation of the data collected in DIS region.

### 2.1 Current Fragmentation in SIDIS at 6GeV

Important issues at low beam energies are the separation of current and target fragmentation regions and the presence of factorization when the quark scattering process and the fragmentation process factorize, and the fragmentation functions depend only on the fractional energy,  $z$ . At low beam energies in DIS the current fragmentation region (CFR) is contaminated with events coming from the target fragmentation region (TFR). A nice graphical representation of different regions as a function of the relevant kinematic variables  $z$ ,  $x_F$  and  $\eta$  is available from Mulders and collaborators. At low  $z$  and  $x_F$  and rapidities  $\eta < 1$  a significant overlap of current and target fragmentation regions is expected (see Fig. 4).

A more quantitative estimate is available from the LUND Monte-Carlo (MC)[43]. The LUND model was successfully used by different experimental groups for different processes and in a wide energy region. Very good agreement of kinematic distributions measured at CLAS and the LUND simulation was shown to take place at energies as low as 4.3 GeV. All this is making the LUND-MC a major tool in SIDIS studies. The relative yield of current fragmentation events extracted from LUND-MC for different beam energies (see. Fig. 5) shows no significant dependence of the CFR fraction on the beam energy in range  $0.8 > z > 0.5$ .

Factorization in the  $z$ -distributions of pions was studied using the 6 GeV data from the CLAS E1 experiment. Distributions of pions in  $z$ , for different  $x$  bins, are shown

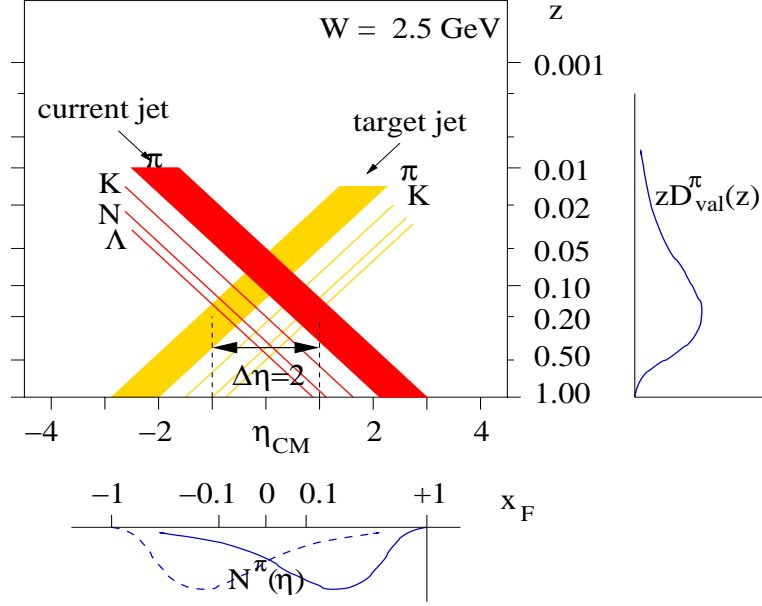


Figure 4: The SIDIS kinematics at  $W = 2.5$  GeV. The kinematic variables are defined as follows:  $z = \frac{E_h}{\nu}$ ,  $x_F = \frac{p_L^*}{p_{Lmax}^*}$  and  $\eta = \frac{1}{2} \ln \frac{E+p_L^*}{E-p_L^*}$  ( $p_L^*$  is the longitudinal momentum of pion in the CM frame).

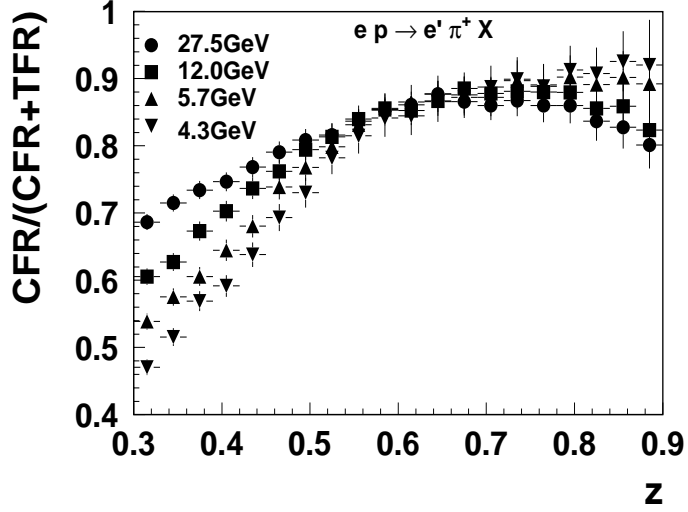


Figure 5: The separation of CFR with  $0.8 > z > 0.5$  is not changing significantly with beam energy.



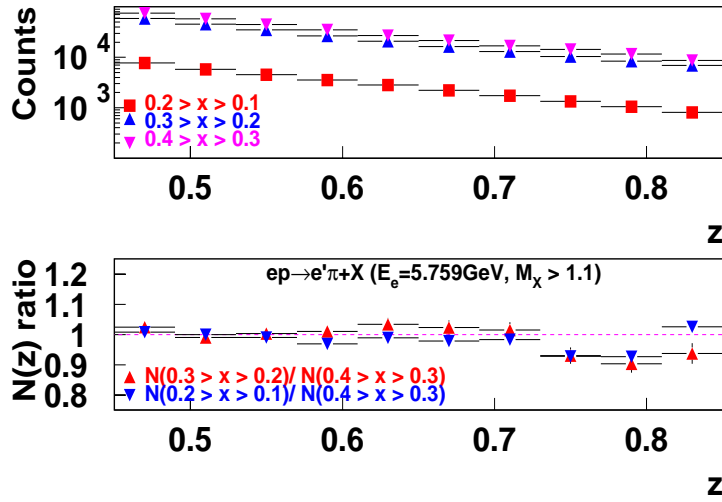


Figure 6:  $z$ -distributions of pions in  $ep \rightarrow e'\pi^+ + X$  for different bins in the  $x$  (top plot) and their ratios (bottom plot) for CLAS E1 data at 6 GeV.

in Fig. 6. No significant dependence within statistical uncertainties was observed in the  $z$ -distributions for different values of  $x$  (bottom plot in Fig.6).

## 2.2 Transversely Polarized Target in CLAS

Two main concerns related to a transversely polarized target in CLAS are the interaction of the transverse target magnet and the CLAS torus, and the behavior of Moller electrons in the transverse field.

Preliminary studies are showing that it is technically possible to run a transversely polarized target at CLAS. Detailed studies of different aspects of transverse target running are under way, including an optimized design of coils, design of a new cryostat for the target, choice of the target material (lithium hydride,  $\text{NH}_3$ ..). A full GEANT simulation is needed to define the shielding from Moller electrons. Chicane magnets will be designed to re-steer the primary electron beam through the transverse field and directing the outgoing beam towards the Faraday cup. The tracking and reconstruction software of CLAS also will need some upgrade to handle the tracks affected by the transverse field.

Kinematic distributions of final state particles were studied using Monte-Carlo generators for DIS and DVCS studies based on the Lund model [43] and DVCS cross sections from Belitsky et al. [55] respectively. Reconstructed (after the standard GEANT simulation, GSIM) events, show reasonable agreement with the e1-6 electroproduction data at 5.7 GeV. Angular distributions of electrons and pions in

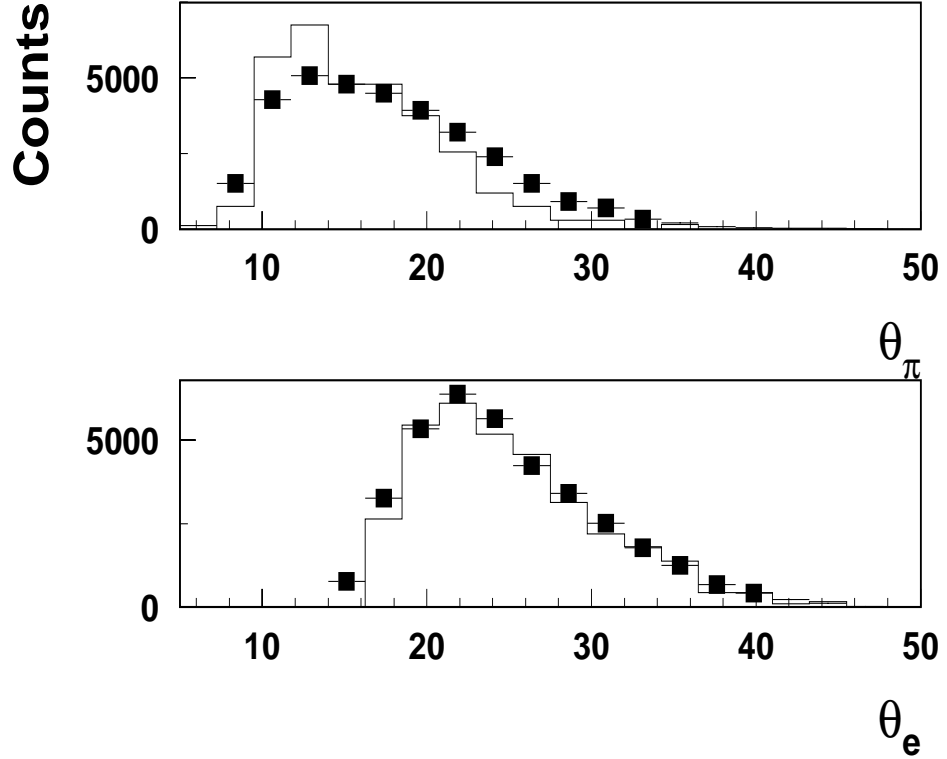


Figure 7: Angular distributions of pions (top plot) and electrons (bottom) in  $ep \rightarrow e'\pi + X$ . The line is for MC-reconstructed events using CLAS DIS Lund MC and squares correspond to the e1-6 data at 5.7 GeV.

$ep \uparrow \rightarrow e'\pi + X$  and electrons photons and protons in  $ep \uparrow \rightarrow e'\gamma + p$  are presented in Figs. 7 and 8 respectively. The kinematic coverage in  $x$  and  $Q^2$  is plotted in Fig. 9.

### 3 Semi-Inclusive Pion SSA

Single-spin asymmetries in SIDIS give access to distribution and fragmentation functions, which cannot easily be accessed in other ways. The list of novel physics observables accessible in SSAs includes the chiral-odd distribution functions, such as the transversity ( $\delta q$ ) [44, 45], the *time-reversal odd* fragmentation functions, in particular the Collins function ( $H_1^\perp$ ) [9], and the recently introduced [8, 46, 13, 14, 15] *time-reversal odd* distribution functions ( $f_{1T}^\perp, h_1^\perp$ ). These latter functions arise from interference between amplitudes with left- and right-handed polarization states,

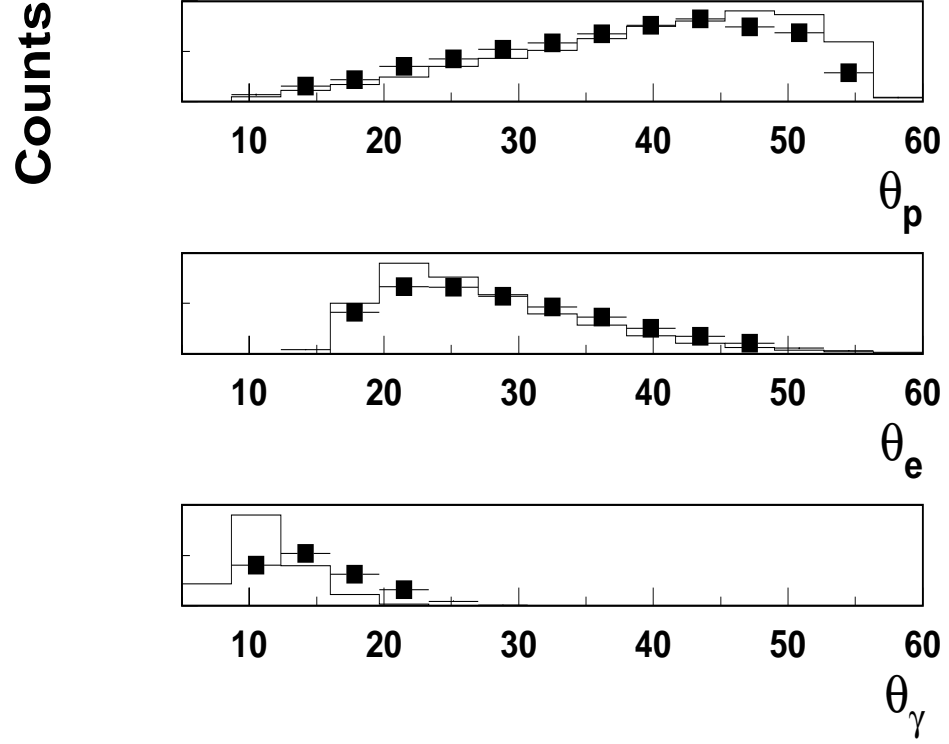


Figure 8: Angular distributions of protons (top plot), electrons, and photons (bottom plot) in  $ep \rightarrow e'\gamma + p$ . The line is for MC-reconstructed events using CLAS DVCS MC based on Belitsky et al [55], and squares correspond to the e1-6 data at 5.7 GeV.

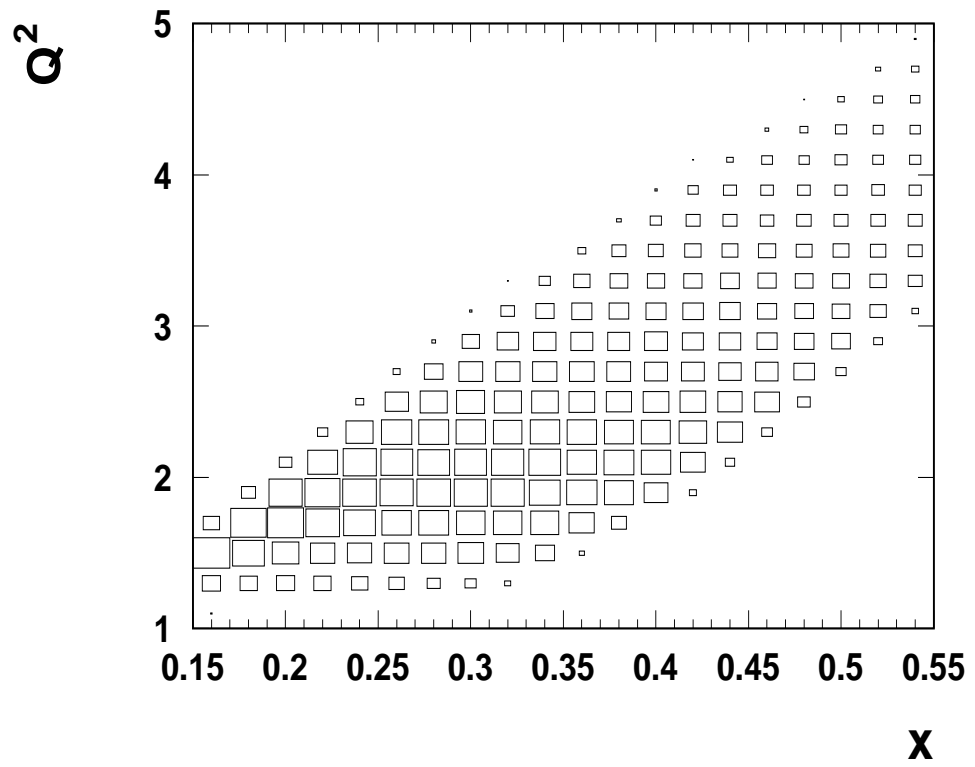


Figure 9: Kinematic coverage of  $ep \rightarrow e'\pi + X$  at 5.7 GeV.

and only exist because of chiral symmetry breaking in QCD. Their study, therefore, provides a new avenue for probing the chiral nature of the partonic structure of hadrons.

Brodsky et al. [13] discussed final state diffractive scattering, which gives rise to interference effects in the DIS cross section[19]. A non-trivial phase structure of QCD amplitudes due to rescattering results in *time-reversal odd* (T-odd) effects and the appearance of single-spin asymmetries at leading twist[13, 14].

The SSA may be related to the distortion of parton distributions in impact parameter space, and can be interpreted in terms of the helicity-flip generalized parton distribution  $E_q(x, 0, -\Delta_\perp^2)$  [17]. The sign and magnitude of the transverse distortion of partons is related to the magnetic properties of the nucleon which is leading to a model-independent prediction for the resulting transverse flavor dipole moments that are of the order of  $0.1 - 0.2$  fm linking SSA and the anomalous flavor-magnetic moment  $\kappa_{q/p}$  in the proton. The physical mechanism that eventually leads to spin asymmetries related to the GPD  $E$  is the final state interaction of the fragmenting quark similar to the Collins mechanism [9].

A detailed study of the  $Q^2$  and  $x_B$  dependencies of SSA as a function of azimuthal angle  $\phi$  and kinematic variables  $y$  and  $z$  would allow the separation of contributions from different mechanisms.

### 3.1 Polarized SIDIS cross section

The total cross section for single pion production by longitudinally polarized leptons scattering off unpolarized protons is defined by a set of structure functions and contains contributions from unpolarized (U) or longitudinally polarized (L) leptons in combination with unpolarized (U), longitudinally polarized (L), or transversely polarized (T) nucleons in the initial state.

$$\frac{d\sigma}{dP_\perp d\phi dx dy dz} = \frac{d\sigma_{UU} + d\sigma_{UL} + d\sigma_{UT} + d\sigma_{LU} + d\sigma_{LL} + d\sigma_{LT}}{dP_\perp d\phi dx dy dz}, \quad (3)$$

The first index refers to the beam polarization and the second one to the target polarization. Up to order  $1/Q$ , only the terms  $\sigma_{UL}$ ,  $\sigma_{UT}$ , and  $\sigma_{LU}$  contribute to the spin-dependent  $\sin\phi$  moments of the cross section [10, 11]. The  $\sigma_{UT}$  ( $\sigma_{UL}$ ) term is proportional to the target polarization component  $S_T$  ( $S_L$ ) transverse (parallel) to the virtual photon momentum.

The kinematics of the process is illustrated in Fig. 10. The angle  $\phi$  is the azimuthal angle between the scattering plane formed by the initial ( $k_1$ ) and final ( $k_2$ ) momenta of the electron or the orientation of the transverse spin and the production plane formed by the transverse momentum of the observed hadron ( $P_\perp$ ) and the virtual photon.

The single-spin terms in the semi-inclusive DIS cross section depend only on the beam polarization  $P_B$  or target polarization  $P_T$ . To extract those terms the cross

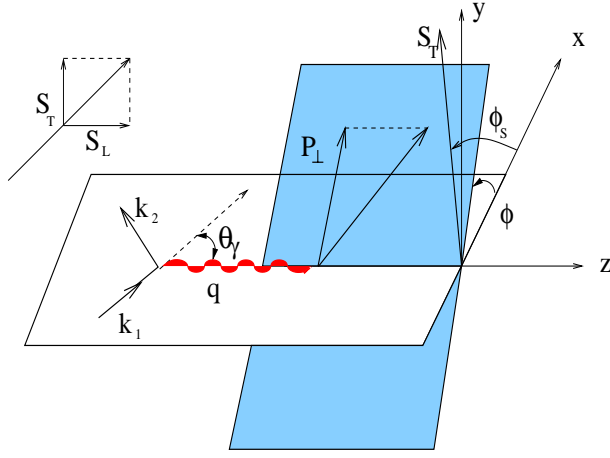


Figure 10: Scattering and production planes and definitions of azimuthal angles.

section could be weighted by the corresponding  $\phi$  dependent functions and integrated over kinematic variables  $\phi$ ,  $y = (E - E')/E$  and  $P_\perp$ , and  $z = E_\pi/(E - E')$  and/or  $x$ .

Full acceptance coverage in  $\phi$  provides redundancy in the data in that the interdependent spin and spatial asymmetries are measured together. The method of extracting the analyzing power was chosen to exploit this redundancy in a way that simplifies the evaluation of the systematic errors. Hence the analyzing powers for target (beam) longitudinal polarization are evaluated as

$$A_{BT}^W = \frac{1}{P_{BT}^+} \frac{\langle \sigma_{BT}^+ \rangle_W}{\langle \sigma_{BT}^+ \rangle_{\sin^2 \phi}} - \frac{1}{P_{BT}^-} \frac{\langle \sigma_{BT}^- \rangle_W}{\langle \sigma_{BT}^- \rangle_{\sin^2 \phi}} \quad (4)$$

where B and T denote the polarization of the beam and target (taking values U and T for unpolarized and transversely polarized case), so  $P_{LU} = P_e$  and  $P_{UT} = P_H$ ,  $\pm$  corresponds to opposite directions of polarization. The weighted cross sections are defined as:

$$\langle \sigma_{BT}^\pm \rangle_W = \int W(\phi) d\sigma^\pm d\phi.$$

The weighting functions  $W(\phi) = \sin \phi$ ,  $\sin 2\phi$ , and  $\sin^2 \phi$  were used to extract the corresponding terms. Thus the SSA in the  $\sin \phi$  moment of the cross section for unpolarized beam and transversely polarized target is defined as:

$$A_{UT}^{\sin \phi} = \frac{\langle \sin \phi \rangle_{UT}}{\langle \sin^2 \phi \rangle_{UT}} = \frac{1}{P^\pm N^\pm} \frac{\sum_{i=1}^{N^\pm} \sin \phi_i}{\sum_{i=1}^{N^\pm} \sin^2 \phi_i}, \quad (5)$$

where  $P^\pm$  and  $N^\pm$  are polarization value and number of events for corresponding polarization state.

Assuming that the quark scattering process and the fragmentation process factorize, and that the fragmentation functions scale and depend only on the fractional

energy,  $z$ , the structure functions could be presented as a convolution of a distribution function and a fragmentation function. Both assumptions have yet to be experimentally confirmed at JLab and HERMES energies for different hard processes.

### 3.2 Transversity and Sivers function

The leading twist transversity distribution  $\delta q$  [44, 45] and its first moment, the tensor charge, are as fundamental for understanding the spin structure of the nucleon as are the helicity distribution  $\Delta q$  and the axial vector charge. The transversity distribution  $\delta q$  is charge conjugation odd, it does not mix with gluons, and for non-relativistic quarks it is equal to the helicity distribution  $\Delta q$ . Thus, it probes the relativistic nature of quarks, and it has a very different  $Q^2$  evolution from  $g_1$ . Its first moment, the tensor charge is reliably calculable in lattice QCD with  $\delta\Sigma = \sum_f \int_0^1 dx (\delta q_f - \delta \bar{q}_f) = 0.562 \pm 0.088$  at  $Q^2 = 2\text{GeV}^2$ , which is twice larger than the proton axial charge [48]. A similar value ( $\delta\Sigma \approx 0.6$ ) was obtained in the effective chiral quark soliton model [49].

At leading twist, the effect of quark transversity can be measured via the azimuthal asymmetry in the fragmentation in SIDIS [9]. For transversely polarized targets, several azimuthal asymmetries already arise at leading order. The following contributions were investigated in Refs. [9, 10, 11, 13, 15, 47]:

$$\begin{aligned} \sigma_{LT}^{\cos\phi} &\propto \lambda_e S_T y (1 - y/2) \cos(\phi - \phi_S) \sum_{q,\bar{q}} e_q^2 x g_{1T}^q(x) D_1^q(z), \\ \sigma_{UT}^{\sin\phi} &\propto S_T (1 - y) \sin(\phi - \phi_S) \sum_{q,\bar{q}} e_q^2 x \delta q(x) H_1^{\perp q}(z), \\ &+ S_T (1 - y + y^2) \sin(\phi + \phi_S) \sum_{q,\bar{q}} e_q^2 x f_{1T}^{\perp q}(x) D_1^q(z), \end{aligned} \quad (6)$$

$$(7)$$

where  $\phi_S$  is the azimuthal angle of the transverse spin in the photon frame, and  $D_1^q(z)$  is the spin-independent fragmentation function.

The first equation for a transversely polarized target describes a double-spin asymmetry giving access to the leading-twist TMD  $g_{1T}^q(x)$  appearing in a convolution with the unpolarized fragmentation function  $D_1^q(z)$  in a  $\cos\phi$  moment of cross section. The latter two equations describe single-spin asymmetries involving the first moments of the T-odd Sivers distribution function and Collins fragmentation function integrated over the transverse momentum of initial and final state quarks, correspondingly.

The  $\sin\phi$  moment of the SIDIS cross section (Eq.7) with a transversely polarized target ( $\sigma_{UT}$ ) [50] contains contributions both from the Sivers effect (T-odd distribution convoluted with  $D_1^q(z)$ ) [8] and the Collins effect (T-odd fragmentation convoluted with transversity) [9].

Contributions to transverse SSAs from T-odd distributions of initial quarks ( $f_{1T}^{\perp q}(x)$  term) and T-odd fragmentation of final quarks ( $H_1^{\perp q}(z)$  term) could be separated

by their different azimuthal and  $z$ -dependencies. The azimuthal angles entering the expression for both contributions are shown in Fig. 11. In case of longitudinally polarized target, the Collins ( $\phi_C$ ) and Sivers ( $\phi_B$ ) angles have opposite sign. Though one can study both contributions measuring the  $\theta_\gamma$  dependence of the target SSA for longitudinal target polarization, the definitive measurement can only be achieved with a transversely polarized target.

Assuming that the transversity of the sea is negligible ( $\delta\bar{q} = 0$ ), and ignoring the non-valence quark contributions in positive pion production, the single-spin transverse asymmetry arising from fragmentation becomes:

$$A_{UT}^{\pi^+} \propto \frac{4\delta u(x)}{4u(x) + \bar{d}(x)} \frac{H_1^{\perp u \rightarrow \pi^+}(z, P_\perp)}{D_1^{u \rightarrow \pi^+}(z, P_\perp)}, \quad (8)$$

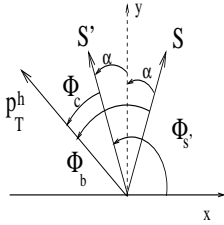


Figure 11: Definition of Collins ( $\phi_C$ ) and Sivers ( $\phi_B$ ) angles. The  $S$  and  $S'$  are initial and final quark polarizations transverse to the virtual photon direction.

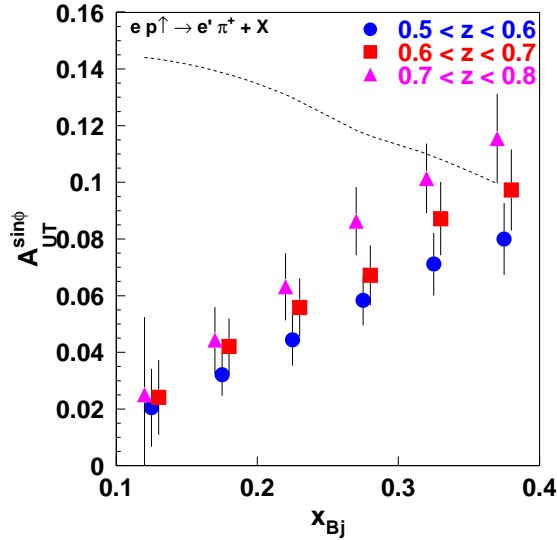


Figure 12: Projected transverse spin asymmetry ( $A_{UT}^{\sin\phi}$ ) due to the Collins effect in single  $\pi^+$  production with CLAS at 5.7 GeV. The line shows the  $x$ -dependence of the contribution from the Sivers effect [13].

The target single-spin asymmetry from polarized quark fragmentation extracted for CLAS kinematics at 6 GeV is plotted in Fig. 12. The estimate was done assuming  $\delta q \approx \Delta q$  and an approximation for the Collins fragmentation function from Ref.[51]. Additional cuts were applied on  $z$  ( $z > 0.5$ ) and the missing mass of the  $e'\pi^+$  system ( $M_X(\pi^+) > 1.3$  GeV). The curves have been calculated assuming a luminosity of  $10^{34}\text{cm}^{-2}\text{s}^{-1}$ , with a  $NH_3$  target polarization of 85% and a dilution factor 0.176, with



2000 hours of data taking. The asymmetry is integrated over all hadron transverse momenta. The extraction of the transversity from  $A_{UT}^{\sin\phi}$  could be performed via Eq. 8 using parameterizations for the unpolarized distribution functions  $u(x)$  and  $\bar{d}(x)$ .

The measurement of transversity is complicated by the presence of an essentially unknown Collins function. Recently, the Collins function for pions was calculated in a chiral invariant approach at a low scale [32], and it was shown that at large  $z$  the function rises much faster than previously predicted [51, 52] in the analysis using the HERMES data on target SSA. It was also pointed out that the ratio of polarized and unpolarized fragmentation is almost scale independent[32]. An important source of extraction of the Collins fragmentation function could be the beam SSA measured for the first time at CLAS [27] and HERMES [36].

The program of transverse asymmetry measurements is underway at HERMES[25] and COMPASS[37].

**Significantly higher statistics of the CLAS data, especially in the large  $x$  region, would enable the extraction of the  $x$  and  $Q^2$  dependencies for different azimuthal moments in a wide kinematical range allowing to reveal the source of the observed SSA and probe the underlying distribution functions.**

## 4 DVCS

Hard electroproduction of real photons (DVCS) is one of the cleanest tools in the problem of constraining GPDs from data. Recently ZEUS [53], H1 [54], HERMES [28] and CLAS [29] collaborations presented first results on DVCS measurements. Consequences of the target and lepton beam polarizations for accessing the generalized parton distributions from experimental measurements of the azimuthal angular dependence of the final state photon or nucleon were presented in Ref. [55]. Several sets of asymmetries, defined as Fourier moments with respect to the azimuthal angle, which allow for a clear separation of the twist-two and -three sectors, were introduced. The differential lepton production cross section was extensively analyzed with power accuracy for all polarization options of the lepton beam and target. It was pointed out that the most favorable physical observables to unravel GPDs from cross sections are spin-azimuthal asymmetries. These asymmetries allow to extract separate components of the angular dependence of the cross section, and in this manner to project out distributions carrying information on the orbital momentum of constituents in the nucleon.

The five-fold cross section for the process  $e(k_1)h(P_1) \rightarrow e(k_2)h(P_2)\gamma(q_2)$  is

$$\frac{d\sigma}{dx dy d|\Delta^2| d\phi d\varphi} = \frac{\alpha^3 xy}{16 \pi^2 Q^2 \sqrt{1 + \epsilon^2}} \left| \frac{\mathcal{T}}{e^3} \right|^2. \quad (9)$$

This cross section depends on the Bjorken variable  $x$ , the squared momentum transfer  $\Delta^2 = (P_2 - P_1)^2$ , the lepton energy fraction  $y$ , and, in general, two azimuthal angles.

The  $\epsilon \equiv 2x\frac{M}{Q}$  and the amplitude  $\mathcal{T}$  is the sum of the DVCS  $\mathcal{T}_{\text{DVCS}}$  and Bethe-Heitler (BH)  $\mathcal{T}_{\text{BH}}$  amplitudes:

$$\mathcal{T}^2 = |\mathcal{T}_{\text{BH}}|^2 + |\mathcal{T}_{\text{DVCS}}|^2 + \mathcal{I}, \quad (10)$$

where  $\mathcal{I}$  is the interference term. This terms can be presented as finite sums of Fourier harmonics:

$$|\mathcal{T}_{\text{BH}}|^2 = \frac{e^6}{x^2 y^2 (1 + \epsilon^2)^2 \Delta^2 \mathcal{P}_1(\phi) \mathcal{P}_2(\phi)} \left\{ c_0^{\text{BH}} + \sum_{n=1}^2 c_n^{\text{BH}} \cos(n\phi) + s_1^{\text{BH}} \sin(\phi) \right\}_{1,1}$$

$$|\mathcal{T}_{\text{DVCS}}|^2 = \frac{e^6}{y^2 Q^2} \left\{ c_0^{\text{DVCS}} + \sum_{n=1}^2 \left[ c_n^{\text{DVCS}} \cos(n\phi) + s_n^{\text{DVCS}} \sin(n\phi) \right] \right\}, \quad (12)$$

$$\mathcal{I} = \frac{\pm e^6}{xy^3 \Delta^2 \mathcal{P}_1(\phi) \mathcal{P}_2(\phi)} \left\{ c_0^{\mathcal{I}} + \sum_{n=1}^3 \left[ c_n^{\mathcal{I}} \cos(n\phi) + s_n^{\mathcal{I}} \sin(n\phi) \right] \right\}, \quad (13)$$

The cross section for a polarized target is given by:

$$d\sigma = d\sigma_{\text{unp}} + \cos(\theta) d\sigma_{\text{LP}}(\Lambda) + \sin(\theta) d\sigma_{\text{TP}}(\varphi), \quad (14)$$

where the polar angle  $\theta$  appears in the decomposition of the spin vector  $S = \cos(\theta)S_{\text{LP}}(\Lambda) + \sin(\theta)S_{\perp}(\Phi)$ . The same decomposition was used for the Fourier coefficients.

The four Compton form factors (CFFs),  $\mathcal{H}, \mathcal{E}, \widetilde{\mathcal{H}}, \widetilde{\mathcal{E}}$  directly accessible from the experiment are given by a convolution of perturbatively calculable coefficient functions and corresponding twist-two GPDs [55]. Eight observables, namely the first harmonics  $\cos(\phi)$  and  $\sin(\phi)$  of the interference term, are accessible in polarized beam and target experiments. Thus, experiments with both longitudinally and transversely polarized target can measure all eight Fourier coefficients  $c_{1,A}^{\mathcal{I}}$  and  $s_{1,A}^{\mathcal{I}}$  and with  $\Lambda = \{\text{unp}, \text{LP}, \text{TP}_x, \text{TP}_y\}$ . Extraction of CFFs using measured azimuthal moments  $c_{1,A}^{\mathcal{I}}$  and  $s_{1,A}^{\mathcal{I}}$  is straightforward:

$$\mathcal{H} = \frac{2-x}{(1-x)D} \left\{ \left[ \left( 2-x + \frac{4x^2 M^2}{(2-x)\Delta^2} \right) F_1 + \frac{x^2}{2-x} F_2 \right] \mathcal{C}_{\text{unp}}^{\mathcal{I}} - (F_1 + F_2) \left[ x \mathcal{C}_{\text{LP}}^{\mathcal{I}} + \frac{2x^2 M^2}{(2-x)\Delta^2} (x \mathcal{C}_{\text{LP}}^{\mathcal{I}} - \mathcal{C}_{\text{TP}+}^{\mathcal{I}}) \right] + F_2 \mathcal{C}_{\text{TP}-}^{\mathcal{I}} \right\}, \quad (15)$$

$$\mathcal{E} = \frac{2-x}{(1-x)D} \left\{ \left[ 4 \frac{1-x}{2-x} F_2 - \frac{4M^2 x^2}{(2-x)\Delta^2} F_1 \right] \mathcal{C}_{\text{unp}}^{\mathcal{I}} + \frac{4xM^2}{(2-x)\Delta^2} (F_1 + F_2) \times (x \mathcal{C}_{\text{LP}}^{\mathcal{I}} - \mathcal{C}_{\text{TP}+}^{\mathcal{I}}) + \frac{4M^2}{\Delta^2} F_1 \mathcal{C}_{\text{TP}-}^{\mathcal{I}} \right\}, \quad (16)$$

$$\widetilde{\mathcal{H}} = \frac{2-x}{(1-x)D} \left\{ (2-x) F_1 \mathcal{C}_{\text{LP}}^{\mathcal{I}} - x(F_1 + F_2) \mathcal{C}_{\text{unp}}^{\mathcal{I}} + \left[ \frac{2xM^2}{\Delta^2} F_1 + F_2 \right] \right\}$$

$$\times \left( x\mathcal{C}_{\text{LP}}^{\mathcal{I}} - \mathcal{C}_{\text{TP}+}^{\mathcal{I}} \right) \Big\}, \quad (17)$$

$$\begin{aligned} \tilde{\mathcal{E}} = \frac{2-x}{(1-x)D} \Big\{ \frac{4M^2}{\Delta^2} (F_1 + F_2) \left( x\mathcal{C}_{\text{unp}}^{\mathcal{I}} + \mathcal{C}_{\text{TP}-}^{\mathcal{I}} \right) + \left[ 4\frac{1-x}{x}F_2 - \frac{4xM^2}{\Delta^2}F_1 \right] \mathcal{C}_{\text{LP}}^{\mathcal{I}} \\ - \frac{4(2-x)M^2}{x\Delta^2}F_1\mathcal{C}_{\text{TP}+}^{\mathcal{I}} \Big\}, \end{aligned} \quad (18)$$

where

$$D = 4 \left( F_1^2 - \frac{\Delta^2}{4M^2} F_2^2 \right) \left( 1 - \frac{\Delta_{\text{min}}^2}{\Delta^2} \right).$$

The real and imaginary parts of  $\mathcal{C}_A^{\mathcal{I}}$  are defined by the corresponding  $\cos(\phi)$  and  $\sin(\phi)$  moments of the interference term ( $c_{1,A}^{\mathcal{I}}$  and  $s_{1,A}^{\mathcal{I}}$ ). The CFFs  $\tilde{\mathcal{E}}$  and  $\tilde{\mathcal{E}}$  are dominated by azimuthal moments  $s_{1,TP\pm}^{\mathcal{I}}$  and  $c_{1,TP\pm}^{\mathcal{I}}$  accessible only with transversely polarized target.

The procedure of extraction of  $\sin(\phi)$  moment through measurement of SSA with unpolarized and polarized targets ( $A_{UT,LU,UL}^{\sin\phi}$ ) is the same as described for SIDIS single-spin asymmetries. The extraction of  $\cos(\phi)$  moments, however, requires detailed Monte-Carlo studies of different  $\cos\phi$  contributions to the CLAS acceptance.

**Transverse target DVCS SSA measurements in addition to unpolarized SSA and longitudinally polarized SSA measurements would provide the full set of data needed for the extraction of CFFs and corresponding GPDs.**

All results known so far on DVCS asymmetries are related to polarized beam and unpolarized target. There are efforts under way at HERMES and CLAS to extract DVCS asymmetries also for the longitudinally polarized target. HERMES[25] and COMPASS[37] are currently planning measurements with transversely polarized targets, but so far no data is available on DVCS asymmetries with a transversely polarized target.

## 5 Hard exclusive Pion SSA

Hard exclusive leptonproduction of a meson  $M$  from a nucleon target  $N$ ,

$$\ell(k_1)N(P_1) \rightarrow \ell'(k_2)N'(P_2)M(q_2) \quad (19)$$

is a promising process to test QCD in exclusive reactions, as well as a means for studies of the properties of nucleon to hadron transitions.

The amplitude for hard exclusive pseudoscalar meson electroproduction off nucleon was calculated in QCD within the leading  $\alpha_s \ln Q^2 / \Lambda_Q^2 CD$  approximation, and significant transverse spin asymmetries were predicted in distributions of final pions [33, 35]. This dependence is especially sensitive to the pion pole dominated spin

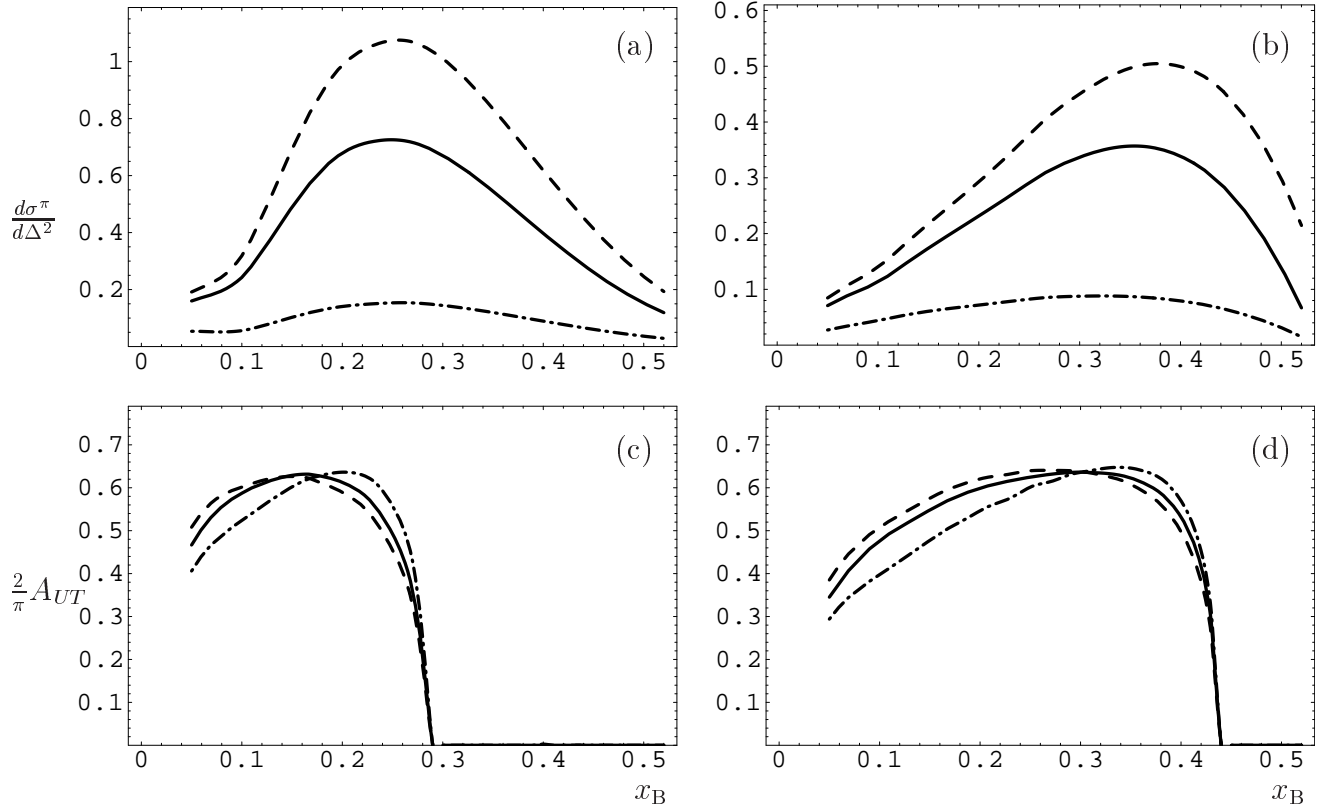


Figure 13: The leading twist predictions for the unpolarized photoproduction cross section  $d\sigma_L^{\pi^+}/d|\Delta^2|$  (in nb/GeV<sup>2</sup>) at  $Q = 10$  GeV<sup>2</sup> [35] are shown for  $\Delta^2 = \Delta_{\min}^2$  and  $\Delta^2 = -0.3$  GeV<sup>2</sup> in the panels (a) and (b), respectively. In (c) and (d) we display the transverse proton single spin asymmetry  $A_{\perp}$  for  $\Delta^2 = -0.1$  GeV<sup>2</sup> and  $\Delta^2 = -0.3$  GeV<sup>2</sup>, respectively. The solid, dashed and dash-dotted curves represent the LO and NLO with the naive and BLM scale setting, respectively [35].

flip GPD  $\tilde{E}$ . It was also argued that the scaling for the spin asymmetry sets in at lower  $Q^2$  than that for the absolute cross section. Perturbative next-to-leading order corrections to the hard exclusive leptonproduction of  $\pi^+$  mesons on a transversely polarized proton target were evaluated by Belitsky and Muller [35]. It was shown that corrections can be large, and there is a significant scale dependence. Even though for the longitudinal polarization of the virtual photon the amplitude is dominated by twist-two contributions the predictions for the cross section suffer from theoretical uncertainties (see Fig. 13a-b). The theoretical uncertainty in the factorization procedure on the amplitude level is translated into large variations of the physical cross section. However, in single-spin asymmetry, given by the ratio of the Fourier coefficients of the cross section, the ambiguities approximately cancel. Thus, the perturbative predictions for this quantity are rather stable. The NLO effects result in  $+7\%$   $-18\%$  corrections to the LO prediction for  $0.1 < x < 0.5$ .

GPD based calculations were performed for the case when the incoming virtual photon is longitudinally polarized. The cross section for transversely polarized photons is suppressed by a power of  $Q[6]$ , but at CLAS energies it may still be significant. Insensitivity to the higher order corrections, is making SSA an appropriate quantity for experimental studies at JLab, and would provide an important test of applicability of GPD based predictions at JLab energies.

The target SSA measured by HERMES [24, 25, 56] in the exclusive limit was the first probe of the transverse SSA. The transverse SSA asymmetry [33, 34, 35] is expected to be large enough to contribute through the small angle of the virtual photon with the proton spin direction (see Fig.10). The data available from polarized  $NH_3$  running with 5.7 GeV at CLAS (EG1 experiment) would allow the extraction of target-SSA as a function of the angle of the virtual photon with the beam direction providing additional information on transverse and longitudinal spin contributions.

**CLAS data on hard exclusive pion production using transversely polarized target would provide a test of the applicability of the GPD formalism at JLab eneries.**

## Summary

Large single-spin asymmetries measured in hard processes both in  $pp$  [22, 23] and  $ep$  [26, 24, 27] scattering are related to the transverse momentum distributions of quarks and probe the elusive OAM. So far known sources of SSA include initial [8, 13, 15] and final [9] state interactions leading to asymmetric distribution and fragmentation of quarks, respectively. SSA in leptonproduction provide access to different 3-dimensional parton distributions (GPDs, IPDs, TMDs) and in particular transversity, Sivers function, and GPDs  $E$  and  $\tilde{E}$  [8, 9, 13, 55]. Unlike cross sections, SSA are proven to be insensitive to a wide class of corrections making them especially appropriate at low beam energies.

The transversely polarized target apart from providing direct access to quark transverse momentum related effect would provide also important missing information needed for the interpretation of longitudinally polarized target measurements.

A key goal of present proposal is the simultaneous measurement of the  $Q^2$  and  $x_B$  dependencies of azimuthal moments (SSA) in the cross section of exclusive and semi-inclusive photon (DVCS) and pion electroproduction off the transversely polarized target, restricting the underlying distribution functions (GPDs, IPDs, TMDs).

## References

- [1] SMC Collaboration (Adeva et al.), Phys. Lett. B 420 (1998) 180.
- [2] HERMES Collaboration (K. Ackerstaff et al.) Phys.Lett. **B464**, 123 (1999).

- [3] EMC Collaboration (Ashman et al.), Phys Lett. B206 (1988) 364.
- [4] X. Ji, Phys. Rev. Lett. **78**, 610 (1997); Phys. Rev. D **55**, 7114 (1997).
- [5] A.V. Radyushkin, Phys. Lett. B **380**, 417 (1996); Phys. Rev. D **56**, 5524 (1997).
- [6] J. C. Collins, L. Frankfurt, and M. Strikman, Phys. Rev. **D56** 2982 (1997).
- [7] D. Soper, Phys. Rev. Lett. **43**, 1847 (1979).
- [8] D. Sivers, Phys. Rev. **D43**, 261 (1991).
- [9] J. Collins, Nucl. Phys. **B396**, 161 (1993).
- [10] P.J. Mulders and R.D. Tangerman, Nucl. Phys. **B461**, 197 (1996).
- [11] A. Kotzinian, Nucl. Phys. **B 441** (1995) 234.
- [12] A. Belitsky, X. Ji and F. Yuan hep-ph/0208038.
- [13] S.Brodsky et al. Phys. Lett. B **530** (2002) 99. hep-ph/0201165.
- [14] J. Collins, hep-ph/0204004.
- [15] X. Ji, F. Yuan e-Print Archive: hep-ph/0206057.
- [16] M. Burkardt, hep-ph/0207047.
- [17] M. Burkardt, hep-ph/0209179.
- [18] M. Diehl, Eur. Phys. J. **C 25**, 223 (2002), hep-ph/0205208.
- [19] S. Brodsky et al., hep-ph/0104291
- [20] S. Brodsky *et al.*, Nucl. Phys. **B 642**, 344 (2002).
- [21] X. Ji, J.-P. Ma, F. Yuan hep-ph/0210430.
- [22] K. Heller et al. 'Proceedings of Spin 96', Amsterdam, Sep.1996,p23
- [23] Fermilab E704 collaboration (A. Bravar et al.), Phys.Rev.Lett. **77**, 2626 (1996).
- [24] HERMES collaboration (A. Airapetyan et al.), Phys.Rev.Lett. **84**, 4047 (2000).
- [25] HERMES collaboration (A. Airapetyan et al.), Phys.Rev. **D64**, 097101 (2001).
- [26] A. Bravar, Nucl. Phys. (Proc. Suppl.) **B79** (1999) 521.
- [27] CLAS Collaboration (H. Avakian et al.) in preparation.

- [28] Hermes Collaboration (A.Airapetian et al), Phys.Rev.Lett. 87, 182001
- [29] CLAS Collaboration (S.Stepanian et al), Phys.Rev.Lett. 87, 182002
- [30] Efremov et. al hep-ph/0001214,Czech.J.Phys Suppl.
- [31] Bo-Qiang Ma *et al.*, hep-ph/0110324.
- [32] A.Bacchetta et.al Phys.Rev., **D65**, 94021 (2002).
- [33] L. Frankfurt *et al.*, Phys. Rev. D **60** 014010, (1999).
- [34] L. Frankfurt, M. Poliakov, M. Strikman and M. Vanderhaeghen, Phys. Rev. Lett., **84** 2589 (2000).
- [35] A. Belitsky and D. Muller, Phys. Lett., **B 513**, 349 (2001).
- [36] A.Miller HERMES Collaboration Proceedings of SPIN2002 BNL,Upton NY 2002.
- [37] COMPASS Collaboration, CERN/SPSLC 96-14.
- [38] H. Avakian Proceedings of SPIN 2002.
- [39] X. Ji, Phys.Rev. **D49**, 114 (1994).
- [40] A. Bachetta and P.J. Mulders, Phys.Rev. **D62**, 114004 (2000).
- [41] Anthony et al., Phys.Rev. Lett. (2002), hep-ph/0204028.
- [42] B. Mecking et al., “The CLAS Detector”, in preparation.
- [43] L. Mankiewicz, A. Schafer and M. Veltri, Comput. Phys. Commun. **71**, 305 (1992).
- [44] J. Ralston and D. Soper, Nucl. Phys. **B152**, 109 (1979)
- [45] R.L.Jaffe and X.Ji Nucl.Phys. **B375** (1992) 527.
- [46] M. Anselmino and F. Murgia, Phys. Lett. B **442** (1998) 470.
- [47] A.M. Kotzinian and P.J. Mulders, Phys. Rev. **D 54** (1996) 1229; Phys. Lett. **B406** (1997) 373.
- [48] E. Leader, A. Sidorov, and D. Stamenov , Phys.Lett. **B462**,189 (1999).
- [49] H. Kim, M. Polyakov, and K. Goike, Phys.Lett. **B387**, 577 (1996).
- [50] D.Boer and P. Mulders, Phys. Rev. **D57**, 5780 (1998).

- [51] A.Efremov, K. Goeke, P. Schweitzer Phys.Lett. **B552**, 37 (2001).
- [52] A. M. Kotzinian *et al.*, Nucl.Phys. **A666**, 290-295 (2000).
- [53] ZEUS collaboration (P.Saull et al.), hep-ex/0003030.
- [54] H1 collaboration (C.Adloff et al.), Phys.Lett. B 517 47, (2001).
- [55] A. Belitsky et al. Nucl. Phys. **B629**, 323 (2002). hep-ph/0105046
- [56] HERMES Collaboration (Airapetian et al.) Phys. Lett. **B535**, 85 (2002).